Time-Optimal Multi-Waypoint Mission Planning in Dynamic Environments

David L. Ferris, Deepak N. Subramani, Chinmay S. Kulkarni, Patrick J. Haley Jr., and Pierre F. J. Lermusiaux*
Department of Mechanical Engineering, Massachusetts Institute of Technology, Cambridge, MA 02139 *Email: pierrel@mit.edu

***Abstract*—The present paper demonstrates the use of exact equations to predict time-optimal mission plans for a marine vehicle that visits a number of locations in a given dynamic ocean current field. This problem bears close resemblance to that of the classic "traveling salesman", albeit with the added complexity that the vehicle experiences a dynamic flow field while traversing the paths. The paths, or "legs", between all goal waypoints are generated by numerically solving the exact time-optimal path planning level-set differential equations. Overall, the planning proceeds in four steps. First, current forecasts for the planning horizon is obtained utilizing our data-driven 4-D primitive equation ocean modeling system (Multidisciplinary Simulation Estimation and Assimilation System; MSEAS), forced by high-resolution tidal and real-time atmospheric forcing fields. Second, all tour permutations are enumerated and the minimum number of times the time-optimal PDEs are to be solved is established. Third, due to the spatial and temporal dynamics, a varying start time results in different paths and durations for each leg and requires all permutations of travel to be calculated. To do so, the minimum required time-optimal PDEs are solved and the optimal travel time is computed for each *leg* of all enumerated tours. Finally, the tour permutation for which travel time is minimized is identified and the corresponding time-optimal paths are computed by solving the backtracking equation. Even though the method is very efficient and the optimal path can be computed serially in real-time for common naval operations, for additional computational speed, a high-performance computing cluster was used to solve the level set calculations in parallel. Our equation and software is applied to simulations of realistic naval applications in the complex Philippines Archipelago region. Our method calculates the global optimum and can serve two purposes: *(a)* it can be used in its present form to plan multi-waypoint missions offline in conjunction with a predictive ocean current modeling system, or *(b)* it can be used as a litmus test for approximate future solutions to the traveling salesman problem in dynamic flow fields.**

I. Introduction

Autonomous underwater vehicles (AUVs) are currently fielded world-wide by commercial companies, militaries, and research institutions, and their use is only set to increase in the coming years (e.g., [1]). For example, signifying the navy's emphasize on unmanned marine systems, the United States Navy has publicly released its Unmanned Underwater Vehicle (UUV) Master Plan and it's AUV Requirements for 2025 [2], [3]. Among the various requirements, "multi-waypoint missions" is a growing area of emphasis from a navigational standpoint for naval operations [4]. In these missions, an AUV visits multiple target locations during a single mission. For such missions, optimally utilizing ocean flow forecasts for navigation can significantly reduce operational costs.

Recent focus of AUV path planning has been on computing exact optimal paths between starting locations and targets in strong and dynamic environments. For this purpose, we developed partial differential equations (PDEs), efficient numerical schemes, and computational systems to compute exact time-optimal paths [5] and energy-optimal paths [6] in strong and dynamic deterministic currents. We also developed stochastic PDEs to compute stochastic time-optimal paths [7] and risk-optimal paths [8] in uncertain ocean currents. We have demonstrated our path planning not only in realistic ocean re-analysis [9], [10], [11], but also in real-time with real AUVs and gliders [12], [13], [14]. Additionally, the theory, schemes and software were also extended for three-dimensional AUV path planning in realistic domains [15] and for optimal ship routing [16], [17].

In the present paper, the goal is to use our planning PDEs to predict time-optimal mission plans for a marine vehicle that visits multiple locations in a dynamic ocean flow field predicted by a data-assimilative ocean modeling system. These missions begin and end in the same location and visit a finite number of waypoints in the minimal time; this problem bears close resemblance to that of the classic "traveling salesman", albeit with the added complexity of a dynamic flow field. Our interest is in finding an exact solution that can serve as a litmus test for future algorithmic solutions.

Previous Progress. Traditionally, the focus of path planning has been on robot motion planning in static environments (e.g., [18], [19]) and recently these have been extended for AUV path planning in dynamic environments. For example, graph search schemes such as modified Dijkstra's algorithm [20], A* search [21], and Rapidly-exploring Random Trees [22] have been used with realistic ocean flows. Other methods such as evolutionary algorithms [23], nonlinear optimization [24], wavefront expansions [25], fast marching methods [26], and LCS-based methods [27] have also been employed for AUV path planning. However, many of these methods are either inexact or computationally expensive in dynamic environments. On the other hand, our PDE-based planning is exact and computationally efficient for strong, dynamic and uncertain flows. We refer the readers to [28], [14] for detailed reviews.

Even though the classic traveling salesman problem and vehicle routing problems are well studied in the field of operations research (e.g., [29], [30]), the literature for Multi Waypoint AUV mission planning has been limited. In ref. [31],

978-1-5386-4814-8/18/$31.00 ©2018 IEEE

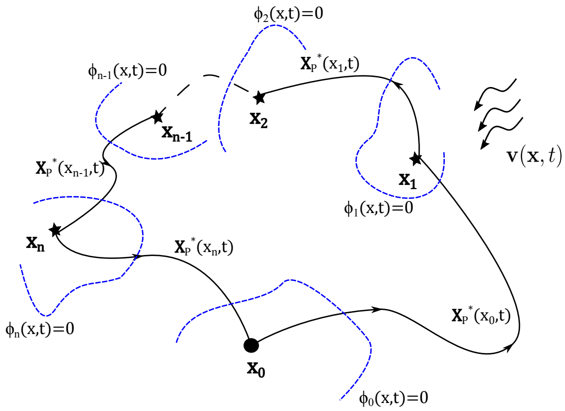

Fig. 1. *Schematic of the multi waypoint time-optimal mission planning problem:* For a vehicle P undertaking a mission in a dynamic flow field $\mathbf{v}(\mathbf{x},t)$, with a start point $\mathbf{x}_0$ and target waypoints $\mathbf{x}_1 \cdots \mathbf{x}_n$, the goal is to compute the time-optimal permutation of waypoints to visit (called a tour) and the time-optimal path for this tour. For any point $\mathbf{x}_i \, \forall i = 0 \cdots n$, $\phi_i(\mathbf{x},t) = 0$ is the reachability front (dashed blue contours) starting at $\mathbf{x}_i$ at the time P reached $\mathbf{x}_i$. The solid black lines $\mathbf{X}^*_P(\mathbf{x}_i,t)$ is the time-optimal path from waypoint i to its next target waypoint. The dotted line between $\mathbf{x}_2$ and $\mathbf{x}_{n-1}$ represents all the time-optimal paths to all waypoints not explicitly shown in this schematic.

the Fast Marching Method for Eikonal equations is applied to solve the continuous traveling salesman problem, but not for realistic ocean currents and vehicles.

II. Theory and Schemes

We formally state the multi waypoint mission planning problem as follows (Fig. 1). Consider a vehicle P navigating in a domain $\mathcal{D}$ indexed by the spatial variable $\mathbf{x}$ and time t. Let $\mathbf{v}(\mathbf{x},t)$ be a strong, dynamic and deterministic flow field in $\mathcal{D}$. Let $\mathbf{x}_0$ be the start point and $\mathbf{x}_i$, where $i = 1 \cdots n$ be n waypoints that are to be visited by P, not necessarily in the said order. We seek the tour (i.e., the permutation of $\{\mathbf{x}_1 \cdots \mathbf{x}_n\}$) that minimizes the total travel time and the time-optimal path of this optimal tour. Note that this travel time may not be unique and there may exist multiple tours with the same net optimal travel time.

A. Multi Waypoint Mission Planning

To compute the exact time-optimal tour and paths, we adopt a four step procedure. First, we obtain the current forecast in the region of interest at the required depth(s) for the planning horizon by utilizing a data-driven 4-D primitive equation ocean modeling system, forced by high-resolution tidal and real-time atmospheric forcing fields such as our Multidisciplinary Simulation Estimation and Assimilation System (MSEAS; [32]). Second, we enumerate all permutations of $\{\mathbf{x}_1 \cdots \mathbf{x}_n\}$ and generate the exhaustive list of complete tours that start and end at $\mathbf{x}_0$ after visiting all $\mathbf{x}_i$ waypoints. Third, for each *leg* of all tours, we utilize the level-set PDEs (sec. II-B) to compute the minimum travel time. Here, the level set equation evolves a reachability front that tracks the set of points that can be reached by a vehicle starting from a point at a given time. Whenever the front reaches a waypoint, a new reachability front is immediately started from that location. This process continues until one set of reachability fronts has reached all goal waypoints and has returned to the original location. Due to the spatial and temporal dynamics, a varying start time results in different paths and durations for each leg and requires all permutations of travel to be calculated. Fourth, the tour for which travel time is minimum is identified. The time-optimal path for the optimum mission is then obtained by solving the backtracking equation.

The above procedure is guaranteed to return the exact time-optimal path for all flows in which the vehicle is controllable at the start and target waypoints. This condition is sufficient to ensure that the optimum travel time between any two waypoints is for the vehicle that leaves the origin waypoint at the earliest time.

B. Compendium of PDE-based Path Planning

The exact time-optimal reachability front of a vehicle P with nominal relative speed $F(t)$, starting at a point $\mathbf{x}_i$ at time t_i in a flow field $\mathbf{v}(\mathbf{x},t)$ is governed by reachability (zero contour of the level-set field $\phi_i(\mathbf{x},t)$) tracking Hamilton Jacobi PDE [5],

$$\frac{\partial \phi_i(\mathbf{x},t)}{\partial t} + F(t)|\nabla \phi_i(\mathbf{x},t)| + \mathbf{v}(\mathbf{x},t) \cdot \nabla \phi_i(\mathbf{x},t) = 0\,, \quad (1)$$

with an initial condition $\phi_i(\mathbf{x},t_i) = |\mathbf{x} - \mathbf{x}_i|$ and open boundary conditions. Here, the optimal arrival time at any target $\mathbf{x}_f$, $T^*(\mathbf{x}_f;\mathbf{x}_i)$, is the first time t for which $\phi(\mathbf{x}_f,t) = 0$. The exact time-optimal paths $\mathbf{X}^*_P(\mathbf{x}_i,t)$ can be computed by solving the particle backtracking equation (when and where ϕ is differentiable),

$$\frac{\mathrm{d}\mathbf{X}^*_P(\mathbf{x}_i,t)}{\mathrm{d}t} = -\mathbf{v}(\mathbf{X}^*_P(\mathbf{x}_i,t),t) - F(t)\frac{\nabla \phi_i(\mathbf{X}^*_P(\mathbf{x}_i,t),t)}{|\nabla \phi_i(\mathbf{X}^*_P(\mathbf{x}_i,t),t)|}\,,$$
$$\mathbf{X}^*_P(\mathbf{x}_i,,T^*(\mathbf{x}_f;\mathbf{x}_i)) = \mathbf{x}_f\,, \quad (2)$$

where $\phi_i(\mathbf{x},t)$ is available from the solution to eq. 1.

In the general case, the vehicle P may not be locally controllable at $\mathbf{x}_i$, (i.e. $F(t) < \mathbf{v}(\mathbf{x},t)$) for a sufficiently long period of time such that $\mathbf{x}$ is no longer in the reachable set at any $t > t_i$ (i.e., $\phi_i(\mathbf{x}_i,t) > 0$). Then, it is sometimes possible to have time-optimal paths by starting from x_i at a time $t_{i,s} > t_i$. Our approach can also compute the exact optimum time-to-go $t_{i,s}$ [5], which can then be used for the present multi waypoint mission planning.

C. Numerical Schemes and Implementation

In the implementation of the multi waypoint mission planning methodology described in Sec. II-A, the first two steps are straightforward. First, we utilize our MSEAS modeling system to forecast the currents in for the planning horizon. Second, we list all combinations of tours. For n waypoints to be visited, the number of possible tours is $n!$ and the number of legs within each tour is $n+1$. Therefore, in the

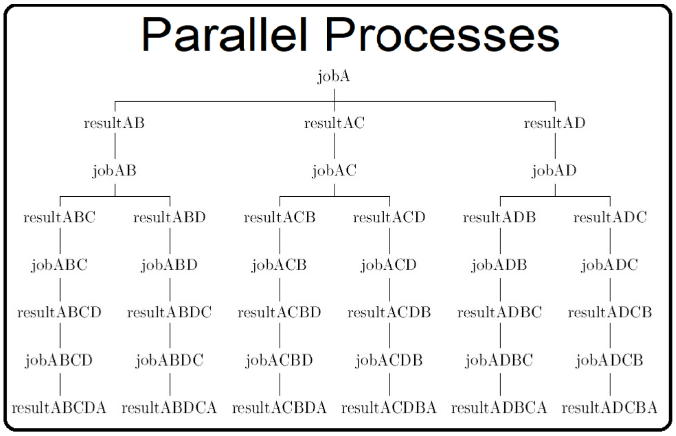

Fig. 2. To improve total mission computation speeds, reachability front calculations are broken down into as many parallel jobs as possible. Any job can start as soon as the results of its preceding job have been saved. This figure demonstrates the job flow for a three-waypoint mission.

third step the planning algorithm has to fill an $n! \times (n+1)$ matrix with the individual leg times and then compute the total time for each tour permutation. Fortunately, since a single reachability front calculation starting from one origin can determine the optimum travel time and paths to all other n waypoints, $n! * (n+1)$ front calculations are not required. In fact, the number of front calculations is given by the recursion, $J_n = 1 + n * J_{n-1}$, where $J_0 = 1$, as seen in Table I.

Even though solving the level-set equation is computationally efficient and the optimal path can be computed serially in real-time for common naval operations, for additional computational speed, a high-performance computing cluster can be used to solve the level set calculations in parallel. However, not all J_n computations can be completed in parallel all at once, as some of them depend on others to determine its start time. Therefore, the maximum number of jobs which can be completed in parallel is equal to the number of tours, $n!$. The benefits of parallel processing increase with the size and discretization of the domain $\mathcal{D}$ (Fig. 1) as well as the number of waypoints. Fig. 2 shows all the 16 reachability front computations that are required for a 3 waypoint mission. All horizontal rows of computations can be accomplished in parallel, and the vertical paths from beginning to end show all possible tours for the mission. We note that several of the tours can be eliminated (pruned) as the computations progress based on the remaining minimum distance, maximum vehicle speed, and maximum ocean currents.

While the number of parallel computations can be equal to the number of tours, there is also a practical limit of how many computations a given computing cluster may process in parallel. Here practical limits of I/O, memory access etc become important. As will be shown in Sec. III, reasonable run times were obtained for up to six waypoint missions processing 720 tours in parallel using the available computing resources.

III. Realistic UUV Mission Planning in Philippines Archipelago Region

We illustrate our theory and distributed implementation by applying it to plan several realistic simulated multi-waypoint missions with progressively increasing waypoints in the Philippines Archipelago region.

The Philippines Archipelago has complex geometry and strong dynamic currents. There are large-scale open ocean dynamics as well as small scale dynamics around islands, through narrow straits, and over steep shelfbreaks [33]. Of the several that we completed, we present two large three-waypoint missions of durations assumed within the range of the U.S. Navy's proposed XLUUV concept (less than 30 days [34]). We also show smaller five and six-waypoint missions within an assumed duration of the U.S. Navy's future LDUUV (less than 5 days [34]).

The first step in our planning is to obtain the current forecasts in the area of operation for the planning horizon. For the present demonstration we re-use the data assimilative multiscale reanalyses from the Philippine Straits Dynamics Experiment 2009 [33] computed using our 2-way nested multi-resolution MSEAS primitive equation modeling system with a nonlinear free-surface [32]. These current fields were also utilized for demonstrating time-optimal path planning in ref. [10]. Here, for the purpose of demonstration, we utilize fields from February 5, 2009. We also assume that the UUV feels the effect of the average horizontal velocity in the top 400 m (or until the local bottom) of the ocean similar to the yo-yo motion of the gliders that we have used in our previous realistic demonstrations [10], [9]. When the UUV is known to travel at a fixed depth, we can modify the currents accordingly as we used in our real time experiments [12].

In Fig. 3 we show the computational domain (within the red bordered box) for our current forecasts and operational areas (M1 to M4 in the black bordered boxes) for the mission planning. The oceanography of the region is described in [33] and a summary of the multiscale currents encountered by the UUVs is provided in ref. [10].

Before we proceed with our realistic missions, we showcase the evolution of all the reachability fronts to compute the two tours of a two way point mission in a small area in the domain away from land to avoid complicating the plots. The local currents here are between 0 and 1 knots of varying direction. A vehicle begins at point A and is tasked to visit points B and C before returning to A. Points B and C are approximately 60 nautical miles and 40 nautical miles, respectively, from the starting point. The vehicle is traveling at 3 knots.

Fig. 4 shows six snapshots in time as the computation of reachability fronts proceeds. Fig. 4a and b show how the initial reachability front grew from point A to points B and C. The front reaches point C first, as shown in the first subfigure. At this point in time, it is possible to plot the time-optimal path between points A and C. The time-optimal path from A to C is plotted in blue with the current along the path represented by the arrows. The color of the path itself corresponds to

TABLE I

COMPUTATIONAL TIME REQUIRED FOR EVALUATING OPTIMAL TRAVEL TIME FOR EACH TOUR. THE TOTAL COMPUTATION TIMES SHOWN ARE BASED ON THE AVERAGE TIME TAKEN TO COMPLETE ONE REACHABILITY FRONT COMPUTATION, $T_{ave} = .5$ HOURS (CORRESPONDING TO THE REALISTIC APPLICATIONS (SEC. III) ON A 3 GHZ QUAD CORE COMPUTE NODE WITH 16GB OF DDR2 RAM AND RUNNING A LINUX OS.

Way-points	Tours	Reachability Front Calculations, $J_n =$	Series Computation Time [hrs], $T_{series} =$	∞-Core Computation Time [hrs], $T_\infty =$	100-Core Computation Time [hrs], $T_{100} =$
n	$n!$	$1 + n * J_{n-1}$	$T_{ave} * J_n$	$T_{ave} * (n+1)$	$approximated$
1	1	2	1	1	1
2	2	5	2.5	1.5	1.5
3	6	16	8	2	2
4	24	65	32.5	2.5	2.5
5	120	326	163	3	4
6	720	1957	978.5	3.5	12.5
7	5040	13700	6850	4	71.5

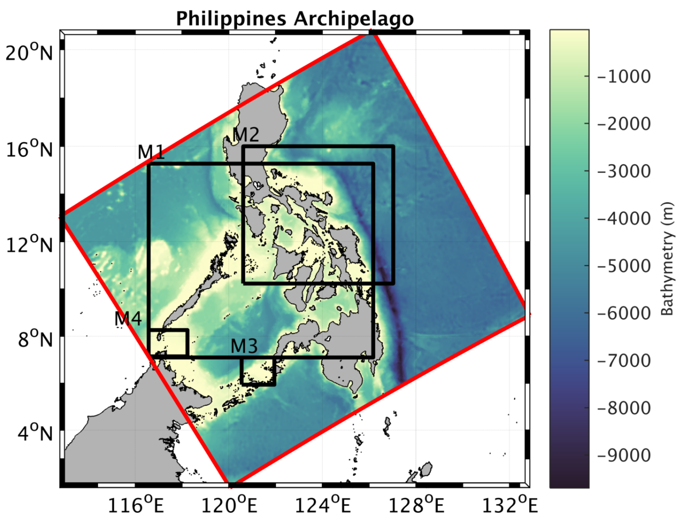

Fig. 3. *Philippines Archipelago Region:* The computational domain in which we forecast the current in shown within the red bordered box and the background is colored with the local bathymetry. Each black bordered box M1 to M4 are regions where Missions 1 to 4 are simulated and zoomed in for later figures (Fig. 5-Fig. 8).

the vehicle's effective velocity while the color of the arrows corresponds to local current velocity.

Fig. 4b shows the original black front continuing to grow while the new green front begins growing from point C. This plot captures the moment the original front reaches point B. Fig. 4c and d continue through time with the path ACBA shown in green and ABCA shown in red. Each plot captures a moment in time where one of the waypoints is reached and a time-optimal path can be shown. Fig. 4e shows the earliest point in time that the mission can complete along the ACBA path. Fig. 4f shows the final time that path ABCA completes.

Next, we consider four realistic mission scenarios with progressively increasing number of waypoints to be visited by our UUV. For each mission we complete the remaining three steps of our planning and report the results.

1) Mission 1: Three Waypoint Shipwreck Inspection from a Central Position: In Mission 1, a vehicle starts from a central position and visits the shipwreck sites of USS PC-1129 near Manila Bay, USS Barbel on the Southern tip of Palawan, and USS Cooper near the Port of Ormoc (area M1 in Fig. 3). By substituting "shipwrecks" with "subsea infrastructure", this could represent mission-type 5 of the RAND survey of UUV Mission, Monitoring Undersea Infrastructure [4].

The targets are located at a straight-line distance of 166, 340, and 196 nautical miles respectively from the starting location. For this simulation, we utilize a constant relative speed of 3 knots to fly the UUV.

Assuming this constant relative speed, the time-optimal tour, ABDCA, completes the mission in 18.83 days and the slowest tour, ADCBA, would take 24.6 hours or 5.4% longer.

The 5% improvement itself is not impressive, but there are several important points to consider about these results. A key takeaway is that the shortest-distance path is not necessarily the fastest. If the optimum order path is run in reverse (ACDBA), the mission would take 22.2 hours (4.9%) longer and is the second slowest time.

Fig. 5 shows it is also important to consider that the overall geography may weigh into path selection. The second fastest path, ACBDA, takes a drastically different route, geographically, avoiding the narrow, complex route between D and C. It may be worth the additional 3.6 hours to avoid this area completely. Additionally, if there is an operational need to avoid the long Northern (B-C) or North-Western (B-D) paths, our planning would reveal the trade-offs in time associated with avoiding those areas.

It should also be pointed out that this mission plan assumes that the underlying current model is accurate. Realistically, lower confidence should be given to the model at times past its predictability limit, and missions this long are most likely beyond what a real-world current model can predict with high accuracy. A vehicle will most likely need to receive updates throughout a mission this long in order to keep on a true optimal path. Finally, a 5% difference between best and worse-case paths means that other factors should be weighed more heavily than just waypoint-order when planning this mission. However, once the waypoint order is decided, there is no reason that these time-optimal paths should not be used.

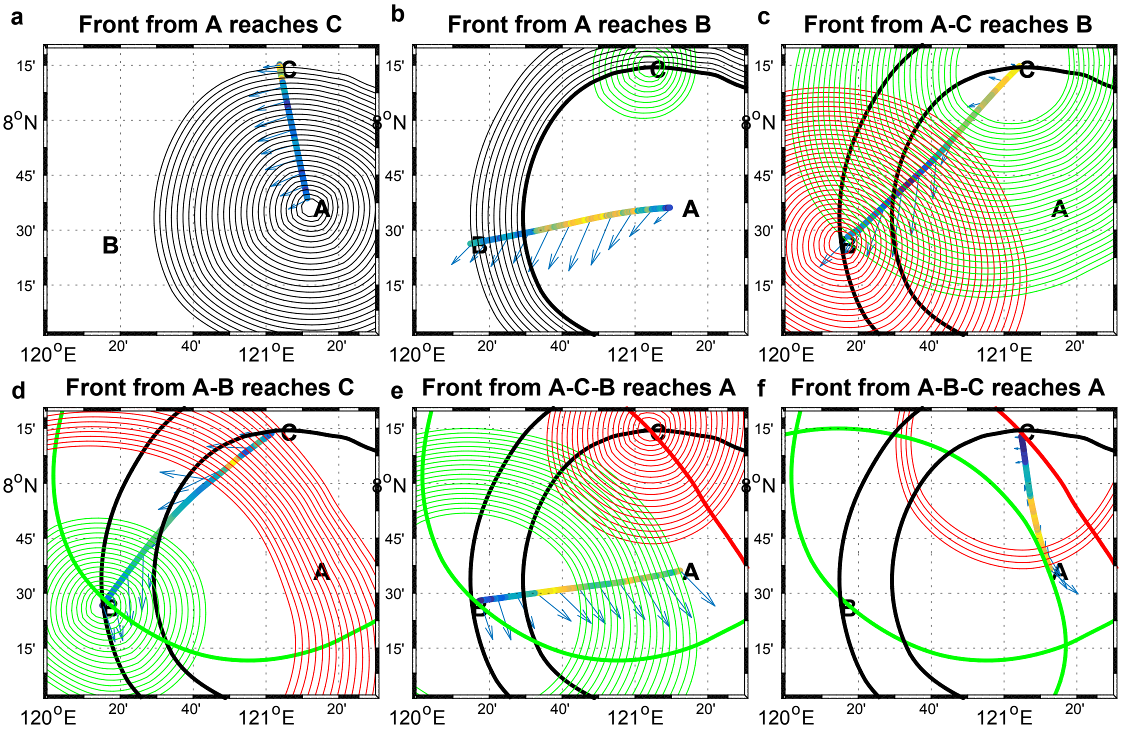

Fig. 4. *Visualizing the evolution of reachability fronts for a two waypoint mission:* (**a**)-(**f**) show how the five reachability front calculations progress through time. The reachability front from A to B & C is shown in black. The remaining calculations are shown in green for tour ACBA and red for tour ABCA. The time-optimal path is shown between points as the colored line where color describes the effective velocity. The paths are overlaid by the local currents encountered along the path.

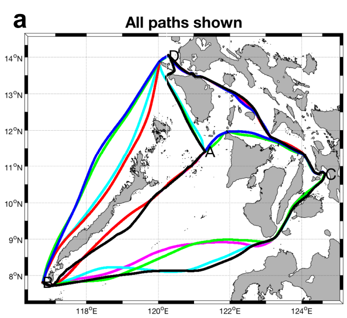

b

Path	Tour Duration (Days)	Hours beyond optimum	% of Optimum*
ADCBA	19.85	24.60	105.4%
ADBCA	19.58	18.00	104.0%
ACDBA	19.75	22.20	104.9%
ACBDA	18.97	3.50	100.8%
ABDCA	**18.83**	**0.00**	**100.0%**
ABCDA	19.40	13.70	103.0%

* Value obtained by dividing tour duration by the minimum tour duration

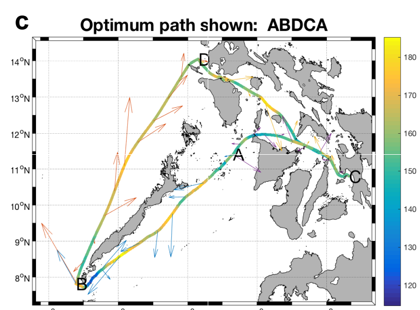

Fig. 5. *Mission 1: Three Waypoint Shipwreck Inspection.* (**a**) Optimal paths of all tours are shown colored by the tour order shown in **b**. (**b**) Duration, hours beyond optimum and travel time of each tour as a percentage of the time-optimal tour. (**c**) The time optimal path of the optimum tour colored by the effective vehicle speed and overlaid by vectors representing the flow encountered along the path.

2) Mission 2: Three Waypoint Shipwreck Inspection from Port of Ormoc: In Mission 2, a vehicle leaves the port of Ormoc and visits the shipwreck sites of USS Ommaney Bay lying West of Panay Island, USS Samuel B. Roberts lying East of the Semirara Islands, and USS Princeton lying east of Lamon Bay (area M2 in Fig. 3). The targets are located at a straight line distance of 200, 110, and 285 nautical miles respectively from the starting location. Assuming a constant, 3 knots, the time-optimal path, ABCDA, completes the mission in 15.80 days and the slowest path, ACBDA, would take 2.35 days (15%) longer.

Fig. 6 shows that the complex geography of the islands forced tight constraints on the vehicle paths. The area where current can be seen to play the biggest role is the divergence of paths from C to D in the Western area. It is also interesting to notice that, depending on the time which the vehicle would pass the small crescent island in the South-Western area (Homonhon Island) the vehicle either went to the East or West of the island.

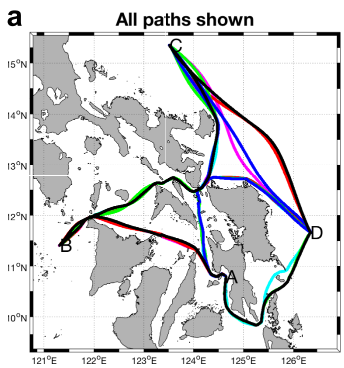

b

Path	Tour Duration (Days)	Hours beyond optimum	% of Optimum*
ADCBA	16.31	12.10	103.2%
ADBCA	18.82	72.40	119.1%
ACDBA	16.80	23.80	106.3%
ACBDA	18.16	56.50	114.9%
ABDCA	17.16	32.50	108.6%
ABCDA	**15.80**	0.00	**100.0%**

* Value obtained by dividing tour duration by the minimum tour duration

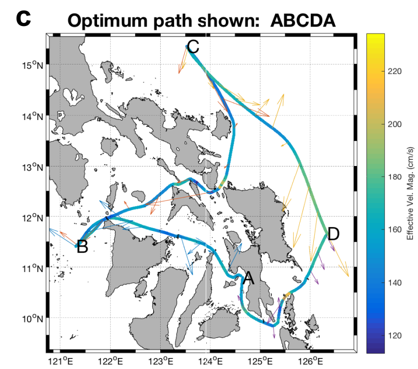

Fig. 6. *Mission 2: Three Waypoint Constrained Route Shipwreck Inspection.* Same as Fig. 5, but for Mission 2.

3) Mission 3: Five Waypoint Harbor Inspection Mission with Varying Start Times: For higher waypoint missions, we focus on LDUUV-type mission scenarios representing mission-type 3 of the RAND survey of UUV missions, near-land and harbor monitoring [4]. Here, we operate in area M3 in Fig. 3 and a UUV is launched from a surface ship (marked with a circle) and inspects five locations within a harbor (marked with stars) as shown in Fig. 7a. The inspection points were laid out in a perfect square with one point in the center, so that there were multiple tours with an identical straight-line distance. By varying the mission start times over the course of a few days, the same mission requires varying optimal paths as shown in Fig. 7.

A five-waypoint mission produces 120 tours, requiring 326 reachability front calculations (Table I) which took a total of 11 minutes to compute on our high performance cluster.

4) Mission 4: Six Waypoint Mine Clearance Mission: The traditional search for mines consists of driving "lawn-mower" patterns, scanning the bottom with active sonar, which is uniquely well accomplished by UUVs as recommended by the RAND survey. There is little for time-optimal path planning to contribute to this lawn-mower process since maintaining straight-line paths supports data collection. However, after processing of the sonar data, and identifying a number of mine-like objects, a follow up mission is normally required for closer inspection and/or neutralization at each location of interest. Mission 4 illustrates a UUV traveling to six randomly placed objects near the Balabac Strait (area M4 in Fig. 3) as shown in Fig. 8 along with the optimal paths. For this mission, the UUV starts its mission from a surface ship (marked by a black circle) approximately 50 nautical miles from the centroid of these objects. All six waypoints (marked by black stars) were randomly placed within a 40 nautical miles by 40 nautical miles square.

There are 720 unique tours possible for a six waypoint mission (Table. I). The total durations of these tours are plotted in Fig. 9. As is expected with many-city traveling salesman problems, there are a few tours which are close to being optimum and a wide range of tour which are nowhere near optimum. The fastest tour duration is 2.26 days while the slowest is 1.38 days (61%) longer. The fastest four tours are highlighted with red stars. The time-optimal paths of these four tours are shown in Fig. 8.

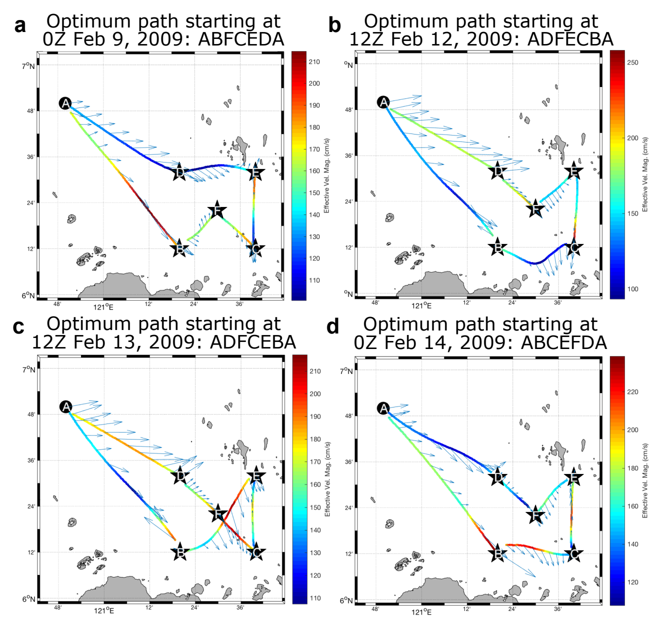

Fig. 7. *Mission 3: Five Waypoint Harbor Inspection Mission with Varying Start Times.* Each path is colored by the effective vehicle speed and overlaid by the currents encountered along the path. (**a**)-(**d**) shows four different optimum tours and paths corresponding to the start time at point A.

All four of these tours result in almost the same duration. The best tour may be the one that investigates a more important area first; the optimal paths for the tour AFGDCBEA (Fig. 8a) would clear the northern shipping route first while the tour AFDCBEGA (Fig. 8c) would leave point G until later in the mission. The best tour may also avoid an enemy sensor or ship, e.g., the optimal path for the tour AGEBCDFA (Fig. 8b) would stay furthest from the island to the South-East, whereas that for tour AFDCGBEA (Fig. 8d) would go very close to this island.

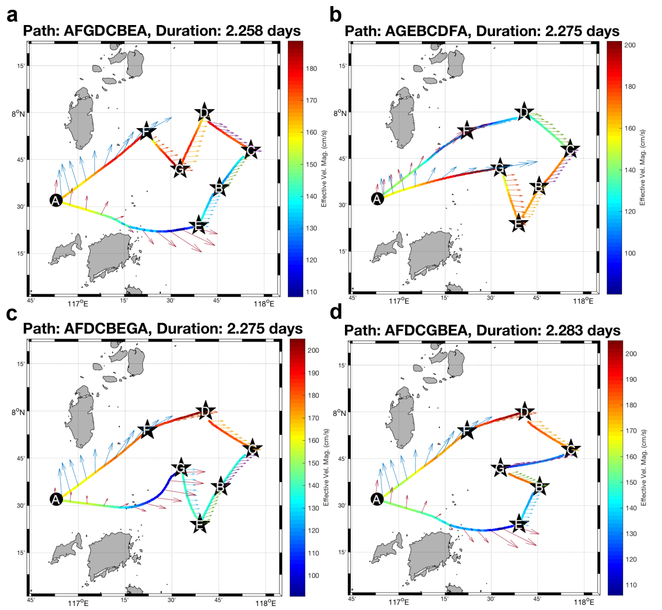

Fig. 8. *Mission 4: Six Waypoint Mine Clearance Mission* Each path is colored by the effective vehicle speed and overlaid by the currents encountered along the path. (**a**)-(**d**) shows four different optimum tours with similar travel times. These correspond to the four tours marked in Fig. 9.

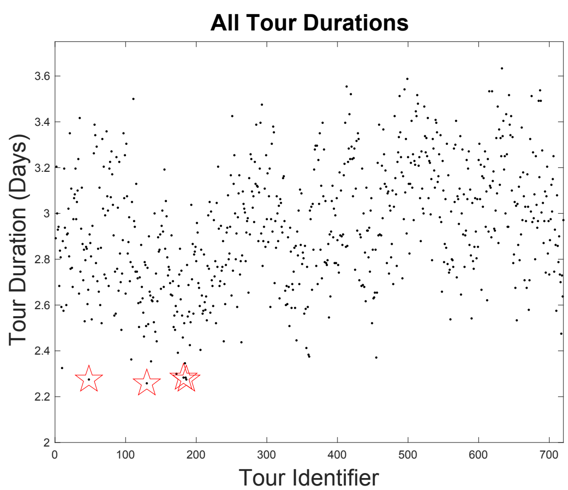

Fig. 9. *Mission 4: Optimal travel times for 720 tours.* The four tours highlighted with red star markers are shown in Fig. 8.

To compute the 720 tour durations, we processed 1957 reachability front calculations in parallel (Table I), and the total processing time was 1 hour and 7 minutes on our computer cluster. This computation time is much smaller than the actual mission durations of 2-3 days. Of course, with more and faster computers, processing speeds for larger real-world mission can be further reduced.

IV. Conclusion

We demonstrated a novel application of exact time-optimal planning PDEs to complete multi-waypoint mission planning in strong and dynamic ocean flows. We laid out the problem statement, theory, and numerical schemes to solve the problem exactly. We then applied our equations and software to compute time-optimal plans for realistic multi-waypoint missions in the complex Philippines Archipelago region. Among the various missions we completed, we highlighted four in the present paper. First, we considered a three waypoint shipwreck inspection from a central position and in the second we completed a similar mission but from the port of Ormoc. These two were longer duration missions with optimal completion times of 18.83 and 15.8 days respectively. The optimal paths avoids the islands in the complex archipelago region and completes their missions by intelligently utilizing the currents to reduce travel times. In the third mission, we considered a five waypoint harbor inspection mission with varying start times. Here we showed that the optimal tours differ with different start times as the dynamic nature of the ocean currents affects the optimal paths between the waypoints. In the fourth mission, we considered a six way point mine clearance mission resulting in 720 tours among which four optimal tours with similar arrival times were selected and presented. Overall, the computational times for all missions were much shorter compared to their mission times. Moreover, the software completes reachability computations in parallel and with more computers, the computational time can be further reduced.

Since our approach calculates the global optimum, it serves two purposes. It can be either used in its present form to plan multi-waypoint missions offline in conjunction with a predictive ocean current modeling system, or it can be used as a litmus test for future algorithmic solutions to the traveling salesman problem in dynamic flow fields.

In the future, service time at the waypoints can also be considered, and time-optimal mission plans can be generated. Also, approximate solutions that utilize heuristics to reduce computational time can be developed. Additionally, this work could be integrated with 3D path planning to account for depth control of the vehicle.

Acknowledgment

We thank the MSEAS group at MIT for insightful discussions. We are grateful to the Office of Naval Research for support under Grants N00014-14-1-0476 (Science of Autonomy - LEARNS), N00014-15-1-2597 (NOPP), N00014-15-1-2616 (DRI-NASCar), and N00014-07-1-0473 (PhilEx) to the Massachusetts Institute of Technology (MIT). We also thank the United States Navy and the MIT-2N program.

References

[1] J. G. Bellingham and K. Rajan, "Robotics in remote and hostile environments," *Science*, vol. 318, no. 5853, pp. 1098–1102, 2007.

[2] *The Navy Unmanned Undersea Vehicle (UUV) Master Plan*, OCLC: 832063493. [Online]. Available: http://oai.dtic.mil/oai/oai?&verb=getRecord&metadataPrefix=html&identifier=ADA511748

[3] United States, Navy, and Undersea Warfare Directorate, *Autonomous undersea vehicle requirement for 2025*, OCLC: 945667105. [Online]. Available: news://usni.org/wp-content/uploads/2016/03/18Feb16-Report-to-Congress-Autonomous-Undersea-Vehicle-Requirement-for-2025.pdf#viewer.action=download

[4] R. W. Button, J. Kamp, T. B. Curtin, and J. Dryden, "A Survey of Missions for Unmanned Undersea Vehicles," 2009. [Online]. Available: https://www.rand.org/pubs/monographs/MG808.html

[5] T. Lolla, P. F. J. Lermusiaux, M. P. Ueckermann, and P. J. Haley, Jr., "Time-optimal path planning in dynamic flows using level set equations: Theory and schemes," *Ocean Dynamics*, vol. 64, no. 10, pp. 1373–1397, 2014.

[6] D. N. Subramani and P. F. J. Lermusiaux, "Energy-optimal path planning by stochastic dynamically orthogonal level-set optimization," *Ocean Modeling*, vol. 100, pp. 57–77, 2016.

[7] D. N. Subramani, Q. J. Wei, and P. F. J. Lermusiaux, "Stochastic time-optimal path-planning in uncertain, strong, and dynamic flows," *Computer Methods in Applied Mechanics and Engineering*, vol. 333, pp. 218–237, 2018.

[8] D. N. Subramani and P. F. J. Lermusiaux, "Risk-optimal path planning in uncertain, strong and dynamic flows," *Ocean Dynamics*, 2017, to be submitted.

[9] D. N. Subramani, P. J. Haley, Jr., and P. F. J. Lermusiaux, "Energy-optimal path planning in the coastal ocean," *Journal of Geophysical Research: Oceans*, vol. 122, pp. 3981–4003, 2017.

[10] T. Lolla, P. J. Haley, Jr., and P. F. J. Lermusiaux, "Time-optimal path planning in dynamic flows using level set equations: Realistic applications," *Ocean Dynamics*, vol. 64, no. 10, pp. 1399–1417, 2014.

[11] ——, "Path planning in multiscale ocean flows: coordination and dynamic obstacles," *Ocean Modelling*, vol. 94, pp. 46–66, 2015.

[12] D. N. Subramani, P. F. J. Lermusiaux, P. J. Haley, Jr., C. Mirabito, S. Jana, C. S. Kulkarni, A. Girard, D. Wickman, J. Edwards, and J. Smith, "Time-optimal path planning: Real-time sea exercises," in *Oceans '17 MTS/IEEE Conference*, Aberdeen, Jun. 2017.

[13] P. F. J. Lermusiaux, P. J. Haley, Jr., S. Jana, A. Gupta, C. S. Kulkarni, C. Mirabito, W. H. Ali, D. N. Subramani, A. Dutt, J. Lin, A. Shcherbina, C. Lee, and A. Gangopadhyay, "Optimal planning and sampling predictions for autonomous and lagrangian platforms and sensors in the northern Arabian Sea," *Oceanography*, vol. 30, no. 2, pp. 172–185, Jun. 2017, special issue on Autonomous and Lagrangian Platforms and Sensors (ALPS).

[14] P. F. J. Lermusiaux, D. N. Subramani, J. Lin, C. S. Kulkarni, A. Gupta, A. Dutt, T. Lolla, P. J. Haley, Jr., W. H. Ali, C. Mirabito, and S. Jana, "A future for intelligent autonomous ocean observing systems," *Journal of Marine Research*, vol. 75, no. 6, pp. 765–813, Nov. 2017, the Sea. Volume 17, The Science of Ocean Prediction, Part 2.

[15] C. S. Kulkarni, "Three-dimensional time-optimal path planning in dynamic and realistic environments," Master's thesis, Massachusetts Institute of Technology, Department of Mechanical Engineering, Cambridge, Massachusetts, Jun. 2017.

[16] G. Mannarini, D. Subramani, P. Lermusiaux, and N. Pinardi, "Evaluation of visir for time-optimal planning in dynamic ocean waves by comparison with differential optimal path planning," *To Be Submitted*, 2018.

[17] P. Lermusiaux, D. Subramani, C. Kulkarni, and P. Haley Jr., "Optimal ship routing in strong, dynamic, and uncertain ocean currents and waves." US Provisional Application, 6 22, 2018.

[18] J.-C. Latombe, *Robot Motion Planning*. New York: Springer Science & Business Media, 2012, vol. 124.

[19] S. M. LaValle, *Planning algorithms*. Cambridge, UK: Cambridge university press, 2006.

[20] G. Mannarini, N. Pinardi, G. Coppini, P. Oddo, and A. Iafrati, "Visir-i: small vessels–least-time nautical routes using wave forecasts," *Geoscientific Model Development*, vol. 9, no. 4, pp. 1597–1625, 2016.

[21] B. Garau, A. Alvarez, and G. Oliver, "Path planning of autonomous underwater vehicles in current fields with complex spatial variability: an A* approach," in *Proceedings of the 2005 IEEE International Conference on Robotics and Automation*. IEEE, 2005, pp. 194–198.

[22] D. Rao and S. B. Williams, "Large-scale path planning for underwater gliders in ocean currents," in *Proceedings of Australasian Conference on Robotics and Automation*, December 2-4 2009, pp. 28–35.

[23] S. Chien-Chou, Y. Yih, H. Mong-Fong, P. Tien-Szu, and P. Jeng-Shyang, "A framework to evolutionary path planning for autonomous underwater glider," in *Modern Advances in Applied Intelligence*, ser. Lecture Notes in Computer Science, M. Ali, J.-S. Pan, S.-M. Chen, and M.-F. Horng, Eds. Springer International Publishing, 2014, vol. 8482, pp. 1–11.

[24] D. Kruger, R. Stolkin, A. Blum, and J. Briganti, "Optimal AUV path planning for extended missions in complex, fast-flowing estuarine environments," in *Robotics and Automation, 2007 IEEE International Conference on*, april 2007, pp. 4265–4270.

[25] M. Soulignac, P. Taillibert, and M. Rueher, "Time-minimal path planning in dynamic current fields," in *IEEE International Conference on Robotics and Automation*, may 2009, pp. 2473 –2479.

[26] J. A. Sethian, "Fast marching methods," *SIAM Rev.*, vol. 41, no. 2, pp. 199–235, Jun. 1999.

[27] M. A. Hsieh, E. Forgoston, T. W. Mather, and I. B. Schwartz, "Robotic manifold tracking of coherent structures in flows," in *IEEE International Conference on Robotics and Automation*. IEEE, 2012, pp. 4242–4247.

[28] P. F. J. Lermusiaux, T. Lolla, P. J. Haley, Jr., K. Yigit, M. P. Ueckermann, T. Sondergaard, and W. G. Leslie, "Science of autonomy: Time-optimal path planning and adaptive sampling for swarms of ocean vehicles," in *Springer Handbook of Ocean Engineering: Autonomous Ocean Vehicles, Subsystems and Control*, T. Curtin, Ed. Springer, 2016, ch. 21, pp. 481–498.

[29] D. L. Applegate, *The traveling salesman problem : a computational study*, ser. Princeton series in applied mathematics. Princeton : Princeton University Press, c2006., 2006.

[30] F. Lam, "Traveling salesman path problems," Thesis, Massachusetts Institute of Technology, 2005. [Online]. Available: http://dspace.mit.edu/handle/1721.1/33668

[31] J. Andrews and J. Sethian, "Fast marching methods for the continuous traveling salesman problem," *Proceedings of the National Academy of Sciences*, vol. 104, no. 4, pp. 1118–1123, 2007.

[32] P. J. Haley, Jr. and P. F. J. Lermusiaux, "Multiscale two-way embedding schemes for free-surface primitive equations in the "Multidisciplinary Simulation, Estimation and Assimilation System"," *Ocean Dynamics*, vol. 60, no. 6, pp. 1497–1537, Dec. 2010.

[33] P. F. J. Lermusiaux, P. J. Haley, W. G. Leslie, A. Agarwal, O. Logutov, and L. J. Burton, "Multiscale physical and biological dynamics in the Philippine Archipelago: Predictions and processes," *Oceanography*, vol. 24, no. 1, pp. 70–89, 2011, Special Issue on the Philippine Straits Dynamics Experiment.

[34] D. Ferris, "Time-optimal multi-waypoint mission planning in dynamic flow fields," Master's thesis, Massachusetts Institute of Technology, Department of Mechanical Engineering, Cambridge, Massachusetts, Jun. 2018.